Review of Laser Doping and its Applications in Silicon Solar Cells

Michelle Vaqueiro-Contreras, Brett Hallam, and Catherine Chan

***Abstract*—Laser-doped selective emitter diffusion techniques have become mainstream in solar cell manufacture covering 60% of the market share in 2022 and are expected to continue to grow to above 90% within the next five years (ITRPV). This was a very rapid uptake of technology, coming from only ∼10% penetration in 2018, and has enabled over 20 fA/cm^2 front recombination current reductions on the dominant passivated emitter and rear cell concepts in the same short period. In this article, a broad overview of key concepts in relation to laser doping methods relevant to solar cell manufacturing is given. We first discuss the basic mechanisms behind laser doping along with the benefits over conventional doping methods. The main laser doping approaches reported in the literature are then discussed, along with implications for metallization strategy, particularly in relation to selective emitter and back surface field formation in the dominant passivated emitter and rear cell technology. Different cell concepts that have benefited from the application of laser doping are also discussed. In the last section, we discuss the main defects induced by laser processing of silicon which affect the finished devices, potential and debated causes, as well as some commonly applied treatments for their mitigation.**

***Index Terms*—Crystalline silicon PV, diffusion processes, laser applications, semiconductor device doping.**

I. Introduction

MODERN laser technology has developed significantly in the past few decades. Fast advances in the understanding and manufacture of lasers have made possible the mass production of a wide variety of high-efficiency light sources in a myriad of wavelengths, pulse shapes/widths, as well as compactness. From an industrial perspective, lasers offer a precise, reliable, and cost-effective substitute to conventionally used processing tools. In the push to higher efficiency industrial silicon solar cells, laser doping has been a particularly important application of laser technology that enables the formation of localized heavily doped regions on a silicon surface, with its main advantages being the following.

1) Room temperature processing, eliminating the need for high-temperature furnaces and so reducing processing time, energy consumption and high thermal budgets on the devices,
2) Localized and fast energy transfer replacing costly photolithography processing and other patterning techniques and
3) Reduction of hazardous chemical usage for doping and etching.

The superiority of laser doping over conventional high-temperature tube furnace annealing has been demonstrated abundantly [1], [2], [3], [4], [5], [6], [7], [8], [9].

Laser doping has become the standard process for forming selective emitters on the front surface of the dominant passivated emitter and rear cell (PERC) technology and can also be used as an elegant process to form the heavily doped p-type back surface fields on their rear surface [10]. It has the potential to also be applied to form the heavily doped contact regions in other high efficiency solar cell technologies, such as n-PERT (passivated emitter rear totally diffused), tunnel-oxide passivated contact (TOPCon) and interdigitated back contact (IBC) cells to name just a few [11].

The principle of laser doping results from a huge power transfer that occurs when a concentrated light beam is focused onto a silicon crystal bringing about a nearly immediate raise of lattice temperature (tens of ns). This temperature can reach levels over 1414 °C which is followed by a likewise fast quenching process (∼735 °C/s) [11]. Such a process, when adequately high energies are utilized, results in the simultaneous rapid melting as well as recrystallisation of laser-subjected locations in the Si crystals, with the crucial benefit of a "near-zero" thermal budget in the rest of the volume. Furthermore, when laser doping is performed in the liquified state, the diffusion coefficient of dopants is orders of magnitude greater than in the solid-state, making dopant diffusion occur in a split second compared to the several-hour processes required using conventional thermal diffusion processes. Manipulation of the laser fluence, wavelength as well as pulse size throughout the doping step can be utilized to finely tune the width and depth of dissolved regions in any type of provided sample for a reliable diffusion or activation of dopants.

The aim of this review article is to provide a broad overview of the laser doping process and how it has been, and can potentially be utilized in silicon solar cells. It will first provide a brief overview on the basic mechanisms of the process, highlighting to the differences and advantages over conventional doping techniques. It will then review applications of laser doping in silicon solar cells, including the most relevant use cases of

Manuscript received 17 August 2022; revised 30 November 2022 and 22 January 2023; accepted 6 February 2023. Date of publication 23 February 2023; date of current version 20 April 2023. This work was supported in part by the Australian Centre for Advanced Photovoltaics (ACAP) under Grant RG200768-B and in part by the Australian Renewable Energy Agency (ARENA) under Grant 2020/RND005. *(Corresponding author: Michelle Vaqueiro-Contreras.)*

The authors are with the University of New South Wales, Sydney, NSW 2052, Australia (e-mail: m.vaqueirocontreras@unsw.edu.au; brett.hallam@unsw.edu.au; catherine.chan@unsw.edu.au).

Color versions of one or more figures in this article are available at https://doi.org/10.1109/JPHOTOV.2023.3244367.

Digital Object Identifier 10.1109/JPHOTOV.2023.3244367

selective emitter and back surface field formation, with emphasis on the industrially dominant PERC cell. Most common dopant sources that have been used for laser doping of solar cells in the literature will be summarized. Specific applications including laser doped semiconductor finger cells, interdigitated back contact cells and potential applications in industrial TOPCon cells will be discussed. Finally, the issue of laser-induced defects and methods to avoid or passivate them will be covered.

II. Conventional Doping and Laser Doping

Conventional techniques for doping of semiconductors such as ion implantation and thermal (gas phase) diffusion have been largely studied throughout the years and are mature technologies. On one hand, ion implantation, the capacity of which was first recognized in 1954, has become one of the most crucial technologies for today's integrated circuit manufacture. Ion implantation has enabled the formation of precise, reliable as well as repeatable doping profiles in semiconductors, along with high tunability in terms of doping focus and depth. Nonetheless, obstacles imposed by the exact control of low-energy ion beams needed for shallow and also sharp joint formation, have represented a considerable disadvantage for its application [12]. Amongst them, damage brought on by very energetic dopants bombardment of the silicon surface which requires additional thermal processing for its elimination as well as dopant activation might result in precipitation, unwanted dopant redistribution, wafer contamination and also surface degradation [13]. The combination of these aspects has hence hampered the advancement of this technology for mainstream solar cell manufacture which overall likewise calls for low cost and high throughput processes.

Thermal diffusions, on the other hand, have been the industrial standard for emitter formation in silicon solar cells since the 1970s. In particular, using phosphorus oxychloride ($POCl_3$) diffusion for electron collector formation on p-type silicon wafers and boron tribromide (BBr_3) on n-type silicon wafers. Both of which have been dominating the market as a result of their low costs, stability and also high throughput, especially in the case of $POCl_3$ diffusions [14]. Despite these perks, optimal thermal diffusions require some rather finetuning of the process and present a series of challenges and drawbacks which need to be addressed.

Thermal diffusion processes begin with the exposure of the silicon wafers to a precursor gas at high temperatures. This usually requires dedicated furnaces to avoid cross-contamination and results in the growth of a phosphorus-rich or boron-rich layer at the silicon surfaces, commonly referred to as phosphosilicate glass (PSG) and borosilicate glass (BSG), respectively. Depending on the dopant species, high-temperature "drive-in" processes are utilized after the dopant layer growth, which enables the diffusion of dopants into the silicon substrate in the solid state. As a result of the differences in diffusion coefficients from the various dopant impurities, the length and temperatures used for junction formation change. A clear example would be that of a boron (B) diffusion, which requires higher temperatures and longer processes when compared to a phosphorus (P) diffusion. A typical B diffusion will take more than 80 mins for junction formation at a temperature of 900–1000 °C [15], whereas P diffusions on the other hand are usually executed at temperatures of 800–900 °C for approximately 50 mins [16]. During the drive-in step, the rich layer dopants present at the surface reach a point of dopant mobility which allow their diffusion into the silicon subsurface. Some of these impurities, once in the silicon crystal, then hop around the silicon atoms and occupy substitutional lattice sites where they become electrically active. Others, however, will instead diffuse to form dopant clusters, precipitates or inhabit interstitial sites, which can bring about severe recombination losses and decreased collection effectiveness of the photogenerated carriers in the so-called "dead layer" [17]. Such dopants are inactive and do not add to the material's conductivity. Process optimization methods such as reduction of $POCl_3$ circulation rates must then be implemented to decrease the concentration of nonactive P, even though a marginal concentration of these impurities is also needed for developing low resistivity contacts making it a sensitive process [18].

Another relevant consideration for thermal diffusions of phosphorus or boron into silicon wafers is the fact that it creates stress on the silicon lattice as an outcome of atomic distance inequality [19]. If not meticulously developed and managed, these stresses can surpass the crucial resolved shear tension, causing the emergence of intrinsic point defect, i.e., diffusion-induced dislocations and vacancies. In addition, thermal diffusion with $POCl_3$ gas inevitably results in huge thermal budgets and the diffusion of dopants across all surfaces of the wafer that are exposed to the gas in the furnace. The former might lead to undesired defect activation while the latter can cause the formation of a diffused region all around the wafer which effectively creates a low resistance path for photogenerated carriers from the front to the rear of the cell, likewise, drastically impacting its performance. Some applied strategies for the isolation consist of additional processing steps such as sawing, grinding, plasma etching, laser ablation, and rear wet etching [20], [21].

Very conveniently, laser doping has emerged to offer a much more flexible approach that overcomes several of the drawbacks presented by conventional diffusion. Even though such flexibility comes at the usual cost of finetuning the laser parameters for each application, they require only a fraction of the time and cost for its optimization compared to thermal diffusions as will be briefly discussed. Much of this optimization comes from the need for precise control of doping depths and shapes. In the case of deep junctions, the depth of the laser doped region heavily depends on the depth of the liquified area in the silicon, whereas the kind of laser used will define the dopant profile. The laser can either be pulsed, such as for Q-switched lasers, where the laser energy is rapidly pulsed, or continuous wave (CW). Pulsed lasers lead to much shallower melting zones typically around 1.5 μm, compared to the $>$10 μm for CW lasers before ablation, and so limiting the depth of the diffusion profile. In the case of short nano-second pulse-length lasers, the silicon commonly solidifies between successive pulses, meaning that the same quantity is re-molten with each pulse, resulting in a more uniform doping profile. Nevertheless, much longer (μs)

pulse length lasers and CW lasers can lead to a much deeper injection of dopants, which can produce better doping profiles under the contacts and better field passivation at the metal/Si interface, as well as junction depths of up to 10 μm. Similar results can be achieved with mode-locked quasi-CW (Q-CW) lasers, which have much shorter (ps) pulse lengths but work at very high frequencies ranging from 80 to 120 MHz which are fast enough to prevent recrystallisation between successive pulses. Another important parameter is the wavelength of the laser. In the case of silicon, the absorption coefficient at 300 K varies by approximately five orders of magnitude across the absorption range, with the best absorption occurring at the lower end of the wavelength spectrum. Still, a wide range of lasers can be used for doping, typically used wavelengths include 355, 532, 1030, and 1064 nm. This is because silicon's absorption coefficient is largely temperature dependent and increases over an order of magnitude at most wavelengths at moderate temperatures ($\sim$700 °C) [22]. Thus, the rapid temperature increase of the silicon substrate during laser exposure accelerates the absorption changes in the whole absorption range, making it important to note that for typical Nd:YAG 532 nm lasers, this increase may lead to extremely shallow absorption and unwanted ablation.

Importantly, laser doping has allowed the easy implementation of selectively diffused surfaces which in the past were only possible using costly and complicated photolithography patterning processes which involved multiple high-temperature diffusion and oxidation steps, as well as many chemical etching steps. This has facilitated the use of lower quality substrates in higher efficiency cell architectures, such as multicrystalline silicon, which is known to degrade during very high-temperature processing [23], [24]. Deeper junctions are able to be formed much faster via laser doping than by conventional diffusion processes, owing to the higher temperatures that can be achieved locally using laser doping, and in many cases, the diffusion of dopants in the liquid state.

III. Laser Doping for Selective Emitter Formation

A. Current Industrial Approach

Current industrial cells opt for the approach of laser doping prior to dielectric deposition, combined with an aligned screen-printed fire-through metallization step [25]. A schematic of this structure is shown in Fig. 1. Laser doping is performed directly after the thermal diffusion step, utilizing either the PSG or BSG layer that forms during diffusion as a source of n-type or p-type dopants, respectively. A wide $\sim$100 μm strip of laser doping is required to facilitate the later alignment of the typical screen-printed metal fingers of 40–50 μm width. The frontal laser doping is performed in the solid state, to avoid melting of the textured pyramid surface and so ensure that the maximum optical absorption is maintained in the nonmetallized regions. After removal of the PSG or BSG layer and deposition of the passivating dielectric layer, an aligned screen-printing and co-firing process is performed. During firing, the metal penetrates through the dielectric layer to contact the underlying laser-doped region. An advantage of this approach is the more effective passivation of laser induced defects, as the passivating dielectric is deposited over the laser doped region. Additionally, laser-induced defects that form due to the thermal expansion mismatch of Si and the dielectric layer are avoided. Using this approach in conjunction with a fire-through metal contacting paste also means the need for a separate local contact opening step is avoided.

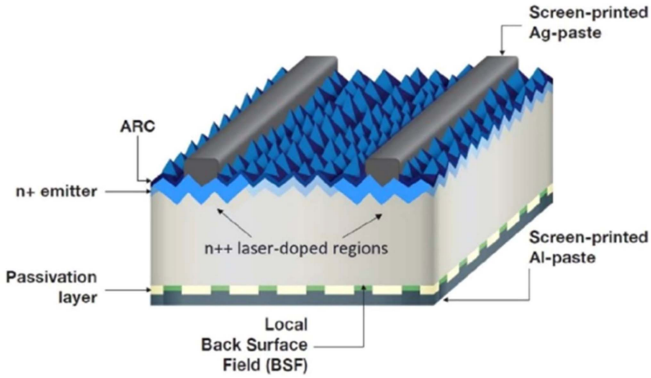

Fig. 1. Schematic of commercial screen-printed LDSE PERC cell. Reprinted from Zhang et al. [26], with permission from IOP Publishing.

B. Laser Doping After Dielectric Deposition

The UNSW developed a laser doping selective emitter (LDSE) approach [27], later commercialized by Suntech Power as PLUTO [28], that involved lasing through a dielectric stack and melting and doping the underlying silicon. In this approach, the dopant source was typically externally deposited through either a spin-on-dopant (SOD) source or using an ultrasonic sprayer [29]. Doped silicon nanoparticle ink [30] or dielectric layers deposited via chemical vapor deposition containing dopant atoms such as phosphorous-doped SiN_x, PSG, and BSG have also been used as the dopant source in a similar approach [29], [31], [32]. Some other viable dielectric stacks are discussed in Section IV. Alternatively, the doping may simply be achieved through redistribution of the dopants in the emitter itself [33]. The laser chemical processing (LCP) method developed by Fraunhofer ISE was typically carried out through a dielectric layer stack in a similar manner to the UNSW approach [34]. In this scenario, the laser was guided by a liquid jet containing a dopant source and so removing the need for a separate step for dopant deposition. One of the main advantages of said methods for laser doping postdielectric deposition is that, if combined with plating, self-aligned metallization is possible as the metal is only deposited on the exposed laser-doped regions. With this approach, laser doping coverage can be kept to a minimum of around 1%–2% (only the laser beam width) compared with the 10% required for alignment tolerance in the current industrial method using screen-printed contacts. The contribution of the laser-doped region to the total emitter recombination current density (J_{0e}) is therefore reduced. Plating is also advantageous as it allows for very fine metallization widths ($<$20 μm), leading to lower shading losses and therefore facilitating more closely spaced fingers and higher sheet resistance emitters. Additionally, plated contacts have much higher conductivity and can achieve

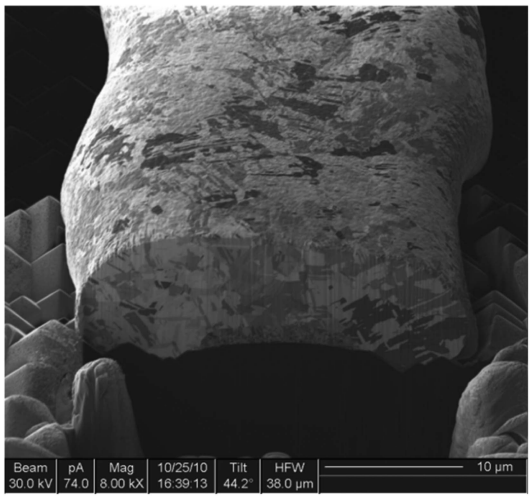

Fig. 2. FIB image of LDSE cell with plated contacts, where laser-doping is performed after dielectric deposition and serving simultaneously as a contact opening process, facilitating a self-aligned plated contact scheme. Reprinted from Hallam et al. [36], with permission from IEEE Electron Devices Society.

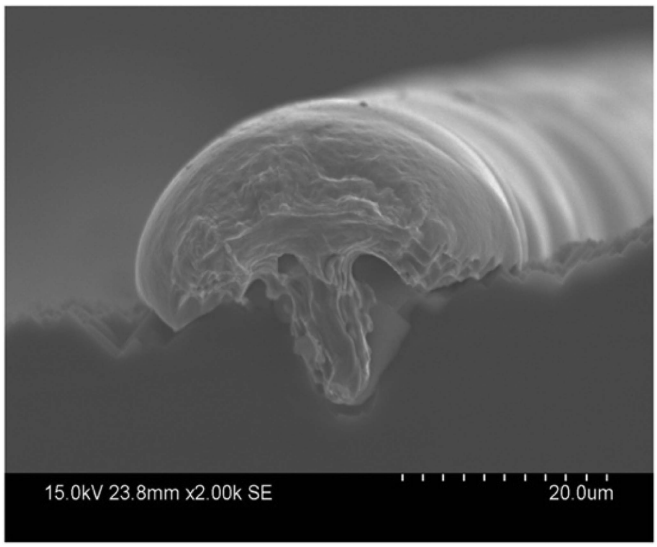

Fig. 3. SEM of laser doped groove with plated contact. Reprinted from Wang et al. [37], with permission from Elsevier.

lower contact resistance than screen-printed contacts, on the order of 0.1 mΩ·cm^2 [35]. A focused ion beam (FIB) image of a cross section of an LDSE cell with plated contacts is shown in Fig. 2 .

At present, however, the widespread commercial use of these self-aligned contacting schemes has been hindered by the challenges presented by this technology including: complexity of process optimization, contact adhesion, diffusion barriers, and waste management. In addition to these, the constant improvements of screen-printing technology such as the capability to form narrower fingers, alignment capabilities, and reduced Ag consumption have made the financial justification of shifting to Cu-based plated contacts more difficult. Therefore, screen-printing continues to be the main contact formation method for LDSE solar cells.

C. Simultaneous Laser Doping and Grooving for Laser Doped and Plated Buried Contacts

An alternative approach developed by Wang et al. [37] involved the formation of narrow (3—5 μm wide), deep (10–15 μm) and heavily doped grooves prior to dielectric deposition (see Fig. 3). Through fine optimization of the laser conditions, silicon is ablated to form the narrow groove whilst simultaneously heavily doping the groove walls with dopants from an SOD source. This approach capitalizes on the benefits of laser doping prior to dielectric deposition, but also facilitates an aligned contacting approach with plating due to the conformal nature of the plasma-enhanced chemical vapor deposition (PECVD) process which enables the groove to largely remain exposed for nucleation of plated metal. This technology achieved efficiencies over 19% for a device with full area aluminum back surface field, further improvements would be expected shifting to a PERC cell structure.

IV. Local Back Surface Field Formation Using Dielectric Films as the Dopant Source

As it has been mentioned, localized doping of controlled dopant concentration and depth are required for advanced and high-efficiency solar cells. Early conventional approaches, therefore, required the application of laborious photolithography or patterning methods in combination with lengthy thermal diffusion sequences and their corresponding chemical removal steps. Furthermore, even when laser doping has been demonstrated as a much more flexible alternative, it still requires the presence of a dopant-containing film which in most cases is added during a previous fabrication step and also requires to be removed after laser processing. If however, the doping species are contained in a pre-existing (and ultimately required) dielectric stack, these extra steps can be eliminated. Such is the case of the standard dielectric stack which forms the rear side of a typical industrial PERC cell, comprising a stack of aluminum oxide (AlO_x) capped with SiN_x. There, the AlO_x is originally present as an excellent surface passivation layer due to its high density of fixed negative charge causing an accumulation effect on p-type silicon surfaces [38], [39]. However, and rather unintendedly, this same layer can act as a rich source of Al, a p-type dopant, for forming heavily doped p^{++} regions in the underlying silicon using laser processing. This has now been demonstrated by several authors [40], [41], [42], [43], [44].

One challenge with laser doping from AlO_x layers, however, is the limited solid solubility of aluminum in silicon above 1200 °C (see Fig. 4). In contrast to boron dopants, the solid solubility of aluminum in silicon peaks at a temperature of ~1100–1200 °C (2×10^{19} cm^{-3}), and then reduces with increasing temperature. The peak active doping concentration using AlO_x-based laser doping may therefore be lower than that when using boron dopants. Although, the use of Al dopants may help to avoid the formation of BO defects in the laser-doped region which is typically oxygen-rich [45].

Despite having a lower solubility limit, Martín et al. demonstrated a p^{++} Al BSF region formed using a 1064 nm Nd:YAG laser with 100 μs pulse length and a dielectric stack of ALD

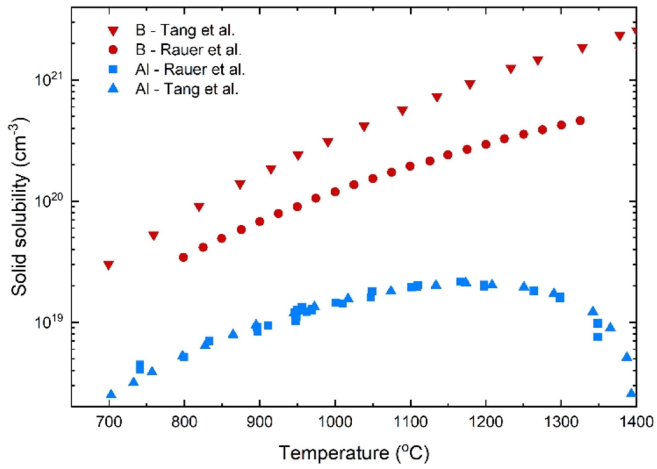

Fig. 4. Solid solubilities of Al and B in crystalline Si as a function of temperature under thermal equilibrium conditions from Rauer et al. [46] and Tang et al. [47].

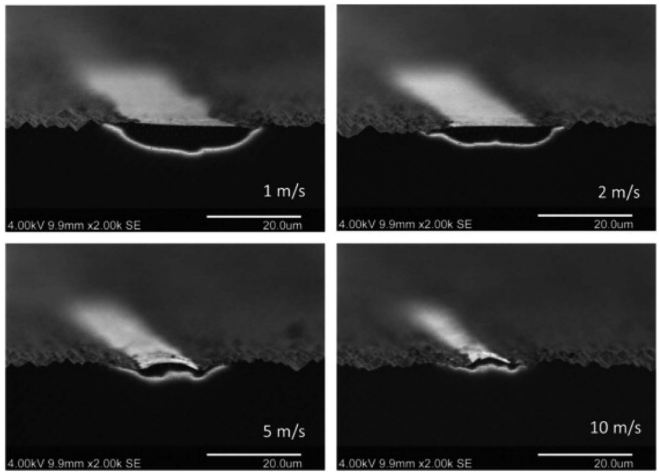

Fig. 5. Combined SEM/EBIC images of laser doped lines formed through Al2O3 at various laser speeds using a 532 nm CW laser. The bright region in the Si bulk indicates the device junction, which extends laterally further than the opening in the dielectric layer. Reprinted from Cornagliotti et al. [55], with permission from Elsevier.

Al_2O_3 and amorphous silicon carbide (a-SiC_x) [43]. Secondary Ion Mass Spectroscopy (SIMS) results indicated a junction depth of 1–2 μm and a peak Al concentration of 5×10^{19} cm^{-3}, which is well above the solid solubility limit shown in Fig. 4, another benefit of laser doping. Sheet resistances were reported to be in the range of 300–400 Ω/sq, significantly higher than expected if all Al atoms in the silicon were electrically active as calculated using EDNA2 [48]. Despite the high sheet resistance, efficiencies over 21% and > 82% fill factors have been achieved, indicative that the laser doped regions were effective as local back-surface-field (LBSF) regions [49].

Following a similar principle, other combinations of dielectric stacks have been reported in the literature including: Al_2O_3/a-SiC_x [49], a-SiN_x:P [50], [51], Al_2O_3/Si_xN_y:B [52], Al_2O_3/a-SiC_x:B [53], and Al_2O_3/a-SiC_x:P [54]. A summary of the reported dielectric layers and stacks in the literature with their corresponding characteristics is shown in Table I. It is shown that sheet resistance values of less than 20 Ω/sq are achievable using this dielectric source method.

One more effective option to utilize Al dopant atoms is by forming a deeper laser doped region through the use of a Q-CW or CW laser (as described in Section II). Using a 355 nm mode locked Q-CW laser, Cornagliotti et al. demonstrated a junction depth of 5 μm for an LBSF region formed by laser doping through a dielectric stack containing a 10 nm thick layer of ALD Al_2O_3 as the dopant source with sheet resistances as low as 9 Ω/sq [55]. A key feature that was noted in that work was that the p^{++} regions formed not only extended deep into the substrate but also laterally beyond the opening in the AlO_x layer (see Fig. 5). This was not observed using an identical process on a wafer with SiN_x passivation layer and boron SOD source. It was hypothesized that the lateral doping beneath the AlO_x layer was due to thermal diffusion of the Al dopants into the silicon from the AlO_x layer in the solid state. This feature could potentially be beneficial in shielding minority carriers from laser-induced defects that form at the edges of the laser openings.

V. Laser Doped Semiconductor Finger Solar Cells

Semiconductor finger solar cells (SFSC) were developed in 2006 as a means to implement a selective emitter structure with screen-printed contacts in production [56]. The SFSC made use of narrow heavily doped channels on the surface of the solar cell running perpendicular to the metal fingers providing a lateral conductive path between the fingers. This meant fingers could be placed further apart with a multitude of resulting benefits including less optical shading, self-aligned screen-print metallization, and reduced metal/Si interface (as the metal fingers only contacted the silicon where they intersected the SFs). Originally the SFs were formed in a similar manner to the buried contact solar cell (laser grooving followed by thermal diffusion), later, laser doping was implemented to form the SFs whereby an SOD was applied, and laser doping was performed through the SiN_x dielectric layer [57], [58], making the technology more commercially viable and also compatible with lower quality wafer types. In the advanced laser-doped semiconductor finger solar cell concept, the SFs were plated with a thin layer of metal after the screen-printed fingers were formed, improving contact resistance at the intersecting points and improving the lateral conductivity of the SFs meaning the screen-printed fingers could be placed further apart again. A schematic of the advanced laser-doped semiconductor finger solar cell is shown in Fig. 6.

VI. Laser Doped Interdigitated Back Contact Cells

IBC cells offer several advantages over conventional cells with contacts on both front and rear, including reduced shading loss and series resistance, decoupling of the optical and electrical optimization, a uniform appearance, a simpler interconnection process, and a higher packing density leading to higher module efficiencies [59].

Despite the high efficiency potential of IBC technology, the complexity of the fabrication process has been a major factor

TABLE I
REPORTED DIELECTRIC STACKS USED AS DOPANT SOURCE FOR LASER DOPING

Stack	Thickness [nm]	Dopant	Rsh_{min} (substrate) [Ω/□]	SRV stack[1] [cm/s]	SRV contact[2] [cm/s]	C_{peak} [/cm^3]	Laser conditions (λ, pulse length)	Refs.
Al_2O_3	20	Al	~ 100 (p-Si)	n/a	n/a	n/a	532 nm, ~ 20 ns	[43]
a-SiN_x:P/n/a	n/a	P	60-100 (p-Si)	< 5	n/a	1×10^{19}	1030 nm, n/a	[50]
SiN_x:P	~75	P	~ 55 (p-Si)	n/a	n/a	8×10^{19}	532 nm, ~ 30 ns	[51]
Al_2O_3/a-SiC_x	50 /50	Al	n/a (p-Si)	< 10	2×10^{3}	n/a	1064 nm, 100 ns	[49]
Al_2O_3/TiO_2	20 /40	Al	~ 250 (p-Si)	n/a	n/a	n/a	534 nm, ~ 20 ns	[41]
Al_2O_3/SiN_x	10-30/80	Al	~ 150 (p-Si)	n/a	1×10^{7}	> 1×10^{21}	532 nm, 9 ps and 355 nm, 20 ns	[42]
Al_2O_3/Si_xN_y:B	1-15 /75	B	< 20 (p-Si)	4	570	n/a	1030 nm, 500-1500 ns	[52]
Al_2O_3/a-SiC_x:B	5-15 /70	Al + B	~ 15 (n-Si)	< 4	4×10^{3}	> 1×10^{20}	1030 nm, 1300 ns	[53]
Al_2O_3/a-SiC_x:P	~100 (combined)	P	n/a (n-Si)	3-15	< 4×10^{3}	2×10^{19}	1030 nm, n/a	[54]
AlO_x/SiN_x/AAO	10 /200 /600	Al + B	< 6 (p-Si)	n/a	n/a	> 1×10^{20}	532 nm, n/a	[40]
Al_2O_3/SiN_x	10 /120	Al	~ 9 (p-Si)	n/a	n/a	4-9×10^{19}	355 nm, 15 ps	[55]
PO_x/Al_2O_3	6 /15	Al + P	35 (n-Si)	n/a	n/a	>1×10^{21}	248 nm, 25 ns	[126]
SiN_x:B	70	B	251 (n+ dif.)	n/a	n/a	>2×10^{20}	308 nm, 150 ns	[127]
SiN_x:P	70	P	~60 (n+ dif.)	n/a	n/a	~7×10^{19}	308 nm, 150 ns	[128]
a-SiC_x:P	30 - 35	P	~40 (p-Si)	10 - 20	< 3×10^{3}	>1×10^{19}	1030 nm, 1 µs	[129]
SiN_x:P	75	P	30 (p-Si)	n/a	n/a	n/a	515 nm, 20 ns	[130]

Note: AAO=Anodic aluminium oxide.
[1]SRV of the stack after thermal processing and before laser.
[2]SRV at lasered contact.

in the limited commercial success of the structure that only accounts for less than 2% of the world's solar cell market share [10]. The low market share is predicted to continue for the next decade, remaining below 5% in the year 2031 [10], largely owing to the high production cost as well as the transition of the industry toward bifaciality for PERC and TOPCon cells instead, which offers a higher potential for cost per watt improvements [60]. The complexity associated with IBC cell fabrication lies in the requirement for regions of both positive and negative polarity to be formed in an interdigitated pattern on the rear of the device and for these regions to be contacted with metal whilst avoiding shunting between positive and negative contacts. The interdigitated pattern has typically been facilitated via high-temperature thermal diffusions either through barrier masks to form selectively diffused layers as in the passivated emitter rear floating junction cell [61], [62], or through the selective removal of a diffused layer after its formation, using methods such as laser ablation or photolithography and wet chemical etching [61], [63], [64], [65]. These methods also typically include the use of high temperature thermal oxidations to form oxide masks. As an example, the interdigitated buried back contact cell developed at UNSW required seven high-temperature diffusion or oxidation steps [66]. In 2004, SunPower commercialized the A300 rear point-contact solar cell concept developed by Stanford University [67] replacing photolithography with screen-printing technology to form the

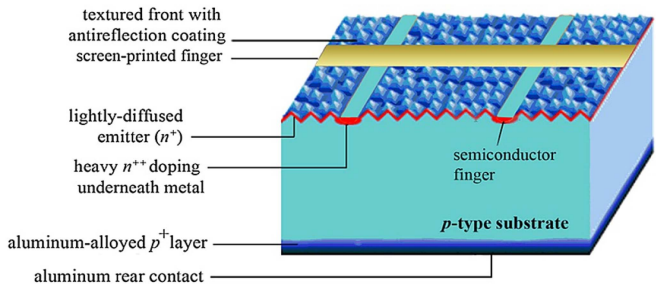

Fig. 6. Advanced laser doped semiconductor finger solar cell. Reprinted with from Mai et al. [58], with permission from Wiley.

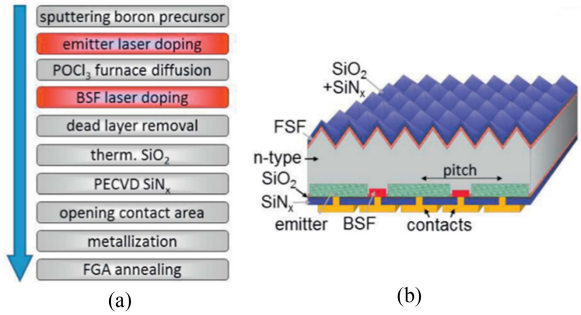

Fig. 7. (a) Process flow and (b) schematic of University of Stuttgart's laser-doped IBC cell. Reprinted from Dahlinger et al. [72], with permission from Elsevier.

patterned diffusion masks, achieving production efficiencies of 21.5% [68]. SunPower now mass produces cells with efficiencies above 24.5% [69] and module efficiencies up to 22.8% [70], although these are typically considered a premium product due to the high lifetime substrates required and the processing that is still relatively complex compared to the more conventional PERC solar cell structure. The use of laser doping in IBC has the potential to significantly simplify the fabrication process of IBC cells further. Replacing high-temperature processing steps with laser doping also facilitates the use of wafer substrates that are sensitive to oxygen precipitation.

In recent years, several research groups have explored the use of laser doping in IBC cells. Most notably, the University of Stuttgart achieved 23.2% efficiency in 2016 where laser doping was used to form both n-type and p-type contacts on the rear, along with laser ablated contact openings to replace photolithography [71] (shown in Fig. 7). To form this cell structure, laser doping was carried out with a sputtered boron dopant source on the rear surface of an n-type wafer to create the p^{++} emitter regions. A $POCl_3$ diffusion was performed to create a high sheet resistivity n-type diffused layer on both sides, the front surface diffusion becoming the front surface field and the rear surface diffusion, and its PSG layer being capitalized on to provide a dopant source for the n^{++} laser doped base contact regions. Following PSG removal, a silicon etch process was performed to remove the phosphorus doped dead layer from each side and remove the possible shunt path between emitter and base. The efficiency of the cell was limited mainly by bulk resistance and bulk recombination, ahead of the losses associated with the laser-doped regions. Other notable examples where laser doping has been utilized in IBC cells are presented in Table II.

Another method of interest that has the potential of simplifying the IBC cell processing even further is the use of laser doping to overcompensate a diffused emitter layer. In this method, dopants of opposite polarity to the diffused surface are introduced via laser doping, in sufficient quantities to overcompensate the diffused surface region and form a contact to the underlying base region of the same polarity. This eliminates the need to selectively remove the diffused layer or perform masked diffusions and enables a high emitter coverage fraction to be maintained, as there is no gap between the p^{++} and n^{++} region. This process was demonstrated by UNSW using a 532 nm CW laser to introduce boron p^{++} regions on phosphorus-diffused p-type wafers [73]. Experimental results indicated that there was minimal tunnel shunting between the heavily doped n^{++} layer and p^{++} LD region [74]. A proof-of-concept IBC cell was demonstrated using this method, whereby both polarities of contacts were formed via laser doping through a rear phosphorus emitter on a p-type substrate [75]. Only a single thermal diffusion step was required which simultaneously formed the rear n^+ emitter region and n^+ floating junction on the front side.

VII. TOPCon Cells

The TOPCon cell structure is currently gaining market share due to the performance enhancements it offers over PERC. In this architecture, the rear surface of the n-type wafer consists of a thin tunnel oxide layer and n-type doped polysilicon layer contacted with silver to form a passivated contact with very low recombination losses. The front surface consists of a homogenously doped boron emitter passivated with a Al_2O_3/SiN_x dielectric stack that acts as the anti-reflection layer. There is a significant discrepancy in the J_0 associated with front and rear surface, with the efficiency of the cell being limited by the front surface design. A selective emitter design would appear a sensible step to drive performance enhancements in TOPCon, with modelling suggesting an efficiency gain of $1\%_{\mathrm{abs}}$ being possible [76].

So far selective boron emitters for TOPCon cells have only been demonstrated in a laboratory setting using chemical etch back approach [77]. In that study, to achieve the low sheet resistances of 65 Ω/sq in the contacted regions a long, energy intensive high-temperature boron diffusion was required. The implementation of the selective emitter resulted in a $0.2\%_{\mathrm{abs}}$ efficiency gain compared to the control devices with a homogenous boron emitter.

The application of laser doping seems to be a logical next step to implementing an industrially relevant process for selective emitter formation on the front surface of a TOPCon cell. The presence of the Al_2O_3 layer lends itself to the possibility of using the Al dopants present in the layer for the laser doping process as discussed in Section IV. However, it remains to be seen whether additional dopant sources would be required due to the limited solid solubility of aluminum in silicon. The potential for a post laser doping anneal at a more favorable temperature for the solid solubility of Al in silicon should be explored as

TABLE II
KEY EXAMPLES OF INTERDIGITATED BACK CONTACT CELLS FABRICATED USING LASER DOPING

Year	Material	Laser	n-type contact	p-type contact	Efficiency	Refs.
2016	n-type Cz	532 nm Nd:YAG	LD: PSG layer	LD: Sputtered boron precursor	23.2%	University of Stuttgart [71]
2017	n-type FZ	248 nm Excimer	LD: P-doped silicon nanoparticle ink	LD: boron spin-on-dopant	22.8%	Australian National University [130]
2015	p-type	1064 nm Nd:YAG	LD: a-SiC_x(n)	LD: ALD Al_2O_3	18.1%	Polytechnic University of Catalonia [131]
2016	n-type	1064 nm Nd:YAG	LD: a-SiC_x(n)	Conventional boron diffusion	20.8%	Polytechnic University of Catalonia [132]
2017	n-type	1064 nm Nd:YAG	LD: a-SiC_x(n)	LD: ALD Al_2O_3	20.4%	Polytechnic University of Catalonia [133]

an option that could be used to activate some of the inactive Al dopants and therefore achieve lower sheet resistances.

VIII. LASER-INDUCED DEFECTS AND PASSIVATION METHODS

Even though laser technology is a very attractive approach for a plethora of applications in silicon photovoltaic manufacture, its application requires a considerable amount of finetuning of laser parameters to reduce the detrimental effects that accompany laser processing. In particular, laser processing can adversely affect device performance by reducing minority carrier lifetime [47], [78], [79], [80], [81], [82], increasing leakage current [78], [83], [84] and diminishing carrier transport [81], all depending on the surface preparation, pre-existing dielectric stacks and the applied laser conditions (pulse duration and energy density). Even though first reports on the effects of laser processing on device performance go back over five decades [83], conclusive identification of some of the introduced point-defects causing much of the diminished device performance and so-called laser-induced defects, is still lacking in the literature. Diverse characterization techniques have been used to investigate the electrical, optical, and structural properties of such defects. Amongst these methods, deep level transient spectroscopy (DLTS) [85], [86], [87], photoconductance decay [78], [80], Hall effect [88], [89], photoluminescence [80], [90], [91], [92], [93], [94], scanning electron microscopy (SEM) [93], transmission electron microscopy [6], [47], [78], [95], [96], [97], SIMS [47], [80], [98] X-ray diffraction [99], and Raman spectroscopy [100], [101], [102] are the most widely applied. From an early stage, studies demonstrated that frequent melting and recrystallization processes caused by the pulsed lasing caused the formation of extended defects in the otherwise perfect lattice as well as the redistribution of nearby impurities. From DLTS

TABLE III
IDENTIFIED LASER DOPING INDUCED DEFECTS

	E1	E2	E3	E4	E5	E6
Assigned chemical species	O-V	V-V	Multi-vacancy centre	V-related		Quenched-in defect (likely recombination centre)
E_T-E_v (eV)	~0.18	~0.25	0.34	0.43	0.53	0.6
Refs.	[112]	[111], [113]	[85], [86]	[85], [114]		[85], [115]

	H1	H2	H3	H4
Assigned chemical species	V-V	V-O-C	V-B	Unclear
E_c-E_T (eV)	~0.22	0.37	0.48	0.6
Refs.	[113]	[109]	[109]	[85], [103]

electrical characterization studies, trap states revealing point defects associated mostly with oxygen-vacancies, divacancies, and some high-order clusters have been reported [87], [100], [103], [104], [105], [106], [107], [108], [109], [110], [111]. However, conclusive identification of most of the formed defects is still lacking and only ambiguous identifications have been reported. In Table III, a summary of the point defects introduced on p-type and n-type silicon upon laser irradiation with their corresponding suggested chemical identities and energy levels

is presented. Similarly, using microscopy techniques, extended defects such as dislocations, micro twins and swirl-like defects have also largely been identified [78], [83], [95], [96], [100]. In addition, some other defects in the form of voids within the bulk of the melted region have also been observed using SEM imaging for slow laser scan speeds when using a CW laser [34]. It was found that void concentration and size increase when low laser speeds are used, although their density was also dependent on the dielectric layers and the deposited dopant source.

In general, however, the nature of the commonly detected defects will greatly depend on two factors, 1) the initial concentration of extrinsic impurities (carbon, oxygen, nitrogen, dopant, etc.), and 2) the degree of structural imperfection of the silicon crystal given that this will directly impact the threshold melting of the material [86].

It is also clear from the literature that significant defect formation is only observed when laser irradiation surpasses the silicon melting threshold which can be regulated by the laser fluence, and that recrystallization velocity is a critical parameter for defect formation. In particular, dislocation density and oxygen introduction have been reported to have an impact on the surface electrical and optical properties of solar cells [94], [116]. Recently, Sun et al. [78] determined that less than 20% degradation of the surface can be attained when restricting the laser-induced dislocation concentration to $\sim 10^6$ cm^{-2}. In that study, the degradation was analyzed in relation to surface carrier lifetime, surface drift mobility, and surface conductivity, while dislocation density was determined using a combination of isotropic etching and SEM imaging.

Several methods for the reduction of laser-induced defects have been reported in the literature. The initially explored and obvious alternative has been the optimization of laser processing conditions, which have been demonstrated to have a strong effect on defect formation [99], [117]. Thermal stress appears to be a significant factor in laser-induced defect formation and can be minimized by reducing the thermal cycling. An easy approach to this is through the use of modified Q-switched lasers or preferably CW or Q-CW lasers [118]. In this way, repeated melting and resolidifying of the silicon between pulses is minimized or avoided, and defect generation often observed along the edge of the laser-doped region can be suppressed [119]. A further benefit arising from the use of CW or Q-CW lasers is the deeper junction formation that is possible, enabling better shielding of minority carriers from the laser-induced defects generated at the surface.

Another source of thermal stress is the thermal expansion mismatch between the silicon and the overlying dielectric layer in the case where laser doping is performed after dielectric deposition [120]. Performing the laser doping prior to dielectric deposition (directly on the silicon surface) can avoid this issue, as discussed in Section III-A. An alternative approach is to modify the dielectric stack to reduce the thermal expansion mismatch through the incorporation of a thin SiO_2 layer between the silicon and SiN_x [1], [45], [119], [121].

Many reports have focused on post-thermal treatments for defect annihilation and hydrogenation. This is because, many of the formed defects have been shown to disappear after thermal treatments in the temperature range 500–700 °C, and to react with atomic hydrogen at temperatures between 100 and 300 °C [86], [106]. Some examples of these include low H ion implantation [122], laser annealing [93], rapid thermal annealing [105], and advanced hydrogenation methods [123], [124], [125]. In practice nonetheless, where laser processing is used for doping and contact opening, defect reduction approaches heavily rely on the application of H-rich dielectric coatings either prior to or postlaser processing, which are often combined with a high-temperature "fast-firing" step depending on the device architecture. For example, the now dominant selective emitter PERC architecture in the industry uses the PSG layer as a dopant source prior to a PECVD SiN_x:H deposition which is carried out at about 400 °C in the presence of hydrogen-containing gases. This mild thermal process and the H-containing dielectric serve as H-plasma treatment and surface passivation of the laser-induced defects all within the same step of the manufacturing process. Following this, the fast-firing process carried out at temperatures between 700 and 900 °C for contact formation after the screen-printing step further annihilates the laser-induced defects while injecting atomic hydrogen to passivate most of the remaining active defects.

IX. Conclusion

Laser-assisted doping of semiconductors has been studied for many decades, and its benefits have been evidenced abundantly in the literature. Progress in the development of faster, cheaper, and more reliable laser sources used in the semiconductor industry has enabled their worldwide adoption. In the silicon-based solar industry, however, it was only in the past half-decade that laser doping became the preferred technology for forming selective emitters on industrial solar cells. This adoption has been driven mainly by the adoption of higher quality silicon wafers resulting from price reductions and the implementation of rear-passivated concepts (PERC/PERT/PERL technologies), which place a higher weight on performance on the surface recombination currents.

Despite the availability of a number of approaches for doping using lasers, the industry-chosen method for selective emitter formation continues to be laser irradiation after the $POCl_3$ gas phase diffusion and prior to dielectric deposition. It may be possible that alternative dopant source methods (e.g., from dielectric layers) become more widely used in the future if plating metallization technologies do increase their market share in the coming years as predicted by the latest ITRPV report, or if laser doping becomes more commonly used to form BSF regions on PERC cells or a selective emitter on the front surface of TOPCon cells. In the case of IBC technology, some of the laser doping advantages have been reduced due to the continuous progress in the now very mature screen-printing technology (tools and pastes) capable of simultaneous doping, which still has the benefits of high throughput and simplicity. It may be that a combination of laser doping technology maturity leading to higher throughputs combined with the much-needed metal reduction consumption in the industry will lead to more widespread adoption.

There is still some work to do in the space of laser-induced defect identification as some of these are still unclear in the

literature, however, several postprocessing approaches have already been adopted to reduce the detrimental impact of these defects via defect annihilation or hydrogen passivation leading to satisfactory results.

Acknowledgment

The authors would like to thank Dr. A. M. Soufiani for sharing his work on laser-induced defects used for the first draft of this manuscript. The views expressed herein are not necessarily the views of the Australian Government, and the Australian Government does not accept responsibility for any information or advice contained herein.

References

[1] B. S. Tjahjono et al., "High efficiency solar cell structures through the use of laser doping," in *Proc. 22nd Eur. Photovolt. Sol. Energy Conf.*, 2007, vol. 3, pp. 966–969.

[2] B. Tjahjono et al., "Application of laser doped contact structure on multicrystalline solar cells," in *Proc. 23rd Eur. Photovolt. Sol. Energy Conf.*, 2008, pp. 1995–2000.

[3] J. Narayan, R. T. Young, R. F. Wood, and W. H. Christie, "p-n junction formation in boron-deposited silicon by laser-induced diffusion," *Appl. Phys. Lett.*, vol. 33, no. 4, Aug. 1978, Art. no. 338, doi: 10.1063/1.90368.

[4] A. Grohe et al., "Novel laser technologies for crystalline silicon solar cell production," *Proc. SPIE*, vol. 7202, pp. 239–250, Feb. 2009, doi: 10.1117/12.810128.

[5] C. W. White et al., "Redistribution of dopants in ion-implanted silicon by pulsed-laser annealing," *Appl. Phys. Lett.*, vol. 33, no. 7, Aug. 1978, Art. no. 662, doi: 10.1063/1.90456.

[6] R. T. Young et al., "Laser annealing of boron-implanted silicon," *Appl. Phys. Lett.*, vol. 32, no. 3, Aug. 1978, Art. no. 139, doi: 10.1063/1.89959.

[7] C. Carlsson, A. Esturo-Bretón, M. Ametowobla, J. R. Köhler, and J. H. Werner, "Laser doping for selective silicon solar cell emitter," in *Proc. 21th Eur. Photovolt. Sol. Energy Conf.*, 2006, pp. 938–940.

[8] Z. Zhou, I. Perez-Wurfl, and B. J. Simonds, "Rapid, deep dopant diffusion in crystalline silicon by laser-induced surface melting," *Mater. Sci. Semicond. Process.*, vol. 86, pp. 8–17, Nov. 2018, doi: 10.1016/J.MSSP.2018.06.012.

[9] M. I. Sánchez et al., "A laser-processed silicon solar cell with photovoltaic efficiency in the infrared," *Physica Status Solidi (A)*, vol. 218, no. 7, Apr. 2021, Art. no. 2000550, doi: 10.1002/PSSA.202000550.

[10] VDMA, Frankfurt am Main, Germany, "International technology roadmap for photovoltaic (ITRPV) 2020 results," 2021.

[11] R. F. Wood, C. W. White, and R. T. Young, *Semiconductors and Semimetals: Pulsed Laser Processing of Semiconductors*. New York, NY, USA: Academic, 1984.

[12] T. M. Liu and W. G. Oldham, "Channeling effect of low energy boron implant in (100) silicon," *IEEE Electron Device Lett.*, vol. 4, no. 3, pp. 59–62, Mar. 1983.

[13] J. Narayan, R. T. Young, and C. W. White, "A comparative study of laser and thermal annealing of boron-implanted silicon," *J. Appl. Phys.*, vol. 49, no. 7, Aug. 1978, Art. no. 3912, doi: 10.1063/1.325398.

[14] H. Li et al., "POCl3 diffusion for industrial Si solar cell emitter formation," *Front. Energy*, vol. 11, no. 1, pp. 42–51, Nov. 2016, doi: 10.1007/S11708-016-0433-7.

[15] R. Basnet et al., "22.6% efficient solar cells with polysilicon passivating contacts on n-type solar-grade wafers," *Sol. RRL*, vol. 3, no. 11, Nov. 2019, Art. no. 1900297, doi: 10.1002/SOLR.201900297.

[16] H. Li, B. Hallam, S. Wenham, and M. Abbott, "Oxidation drive-in to improve industrial emitter performance by POCl3 diffusion," *IEEE J. Photovolt.*, vol. 7, no. 1, pp. 144–152, Jan. 2017.

[17] B. Min et al., "Heavily doped Si:P emitters of crystalline Si solar cells: Recombination due to phosphorus precipitation," *Physica Status Solidi, Rapid Res. Lett.*, vol. 8, no. 8, pp. 680–684, Aug. 2014, doi: 10.1002/PSSR.201409138.

[18] A. Dastgheib-Shirazi et al., "Relationships between diffusion parameters and phosphorus precipitation during the POCl3 diffusion process," *Energy Procedia*, vol. 38, pp. 254–262, Jan. 2013, doi: 10.1016/J.EGYPRO.2013.07.275.

[19] P. J. Cousins and J. E. Cotter, "The influence of diffusion-induced dislocations on high efficiency silicon solar cells," *IEEE Trans. Electron Devices*, vol. 53, no. 3, pp. 457–464, Mar. 2006.

[20] A. Reinders, P. Verlinden, W. van Sark, and A. Freundlich, *Photovoltaic Solar Energy: From Fundamentals to Applications*. Hoboken, NJ, USA: Wiley, 2017.

[21] A. Hauser et al., "Comparison of different techniques for edge isolation," in *Proc. 17th Eur. Photovolt. Sol. Energy Conf.*, 2001, pp. 1739–1742.

[22] G. E. Jellison and F. A. Modine, "Optical absorption of silicon between 1.6 and 4.7 eV at elevated temperatures," *Appl. Phys. Lett.*, vol. 41, no. 2, Aug. 1998, Art. no. 180, doi: 10.1063/1.93454.

[23] S. P. Phang, W. Liang, B. Wolpensinger, M. A. Kessler, and D. MacDonald, "Tradeoffs between impurity gettering, bulk degradation, and surface passivation of boron-rich layers on silicon solar cells," *IEEE J. Photovolt.*, vol. 3, no. 1, pp. 261–266, Jan. 2013.

[24] I. Hanke, M. Apel, and W. Schroter, "Influence of annealing conditions of recombination properties and diffusion length in cast multicrystalline silicon for solar cells'," in *Proc. 14th Eur. Photovolt. Sol. Energy Conf.*, 1997, pp. 735–738.

[25] F. Miao, S. Zhang, W. Lian, B. Zhao, and Q. Wei, "Improvement of PERC solar cell efficiency based on laser-doped selective emitter," *AIP Conf. Proc.*, vol. 2147, no. 1, 2019, Art. no. 40011, doi: 10.1063/1.5123838.

[26] Y. Zhang, L. Wang, D. Chen, M. Kim, and B. Hallam, "Pathway towards 24% efficiency for fully screen-printed passivated emitter and rear contact solar cells," *J. Phys. D, Appl. Phys.*, vol. 54, 2021, Art. no. 214003, doi: 10.1088/1361-6463/abe900.

[27] S. R. Wenham and M. A. Green, "Self aligning method for forming a selective emitter and metallization in a solar cell," WO 00/01019, 2002.

[28] Z. Wang et al., "Advanced PERC and PERL production cells with 20.3% record efficiency for standard commercial p-type silicon wafers," *Prog. Photovolt., Res. Appl.*, vol. 20, no. 3, pp. 260–268, 2012, doi: 10.1002/pip.2178.

[29] T. Li et al., "Laser-doped solar cells exceeding 18% efficiency on large-area commercial-grade multicrystalline silicon substrates," *Prog. Photovolt., Res. Appl.*, vol. 21, no. 6, pp. 1337–1342, 2013, doi: 10.1002/pip.2292.

[30] M. Ernst, D. Walter, A. Fell, B. Lim, and K. Weber, "Efficiency potential of P-type Al2O3/SiNx passivated PERC solar cells with locally laser-doped rear contacts," *IEEE J. Photovolt.*, vol. 6, no. 3, pp. 624–631, May 2016.

[31] B. Terheiden, "CVD boron containing glasses – an attractive alternative diffusion source for high quality emitters and simplified processing - a review," *Energy Procedia*, vol. 92, pp. 486–492, Aug. 2016, doi: 10.1016/J.EGYPRO.2016.07.131.

[32] M. Heilig, J. Engelhardt, G. Hahn, and B. Terheiden, "Comparison of laser-doped emitters from as-deposited and thermally diffused APCVD doping glasses on silicon substrates," *AIP Conf. Proc.*, vol. 2147, no. 1, Aug. 2019, Art. no. 070004, doi: 10.1063/1.5123865.

[33] B. Hallam et al., "Efficiency enhancement of i-PERC solar cells by implementation of a laser doped selective emitter," *Sol. Energy Mater. Sol. Cells*, vol. 134, pp. 89–98, 2015, doi: 10.1016/j.solmat.2014.11.028.

[34] D. Kray et al., "Laser chemical processing (LCP)—A versatile tool for microstructuring applications," *Appl. Phys. A*, vol. 93, no. 1, 2008, Art. no. 99, doi: 10.1007/s00339-008-4723-8.

[35] B. Min et al., "A roadmap toward 24% efficient PERC solar cells in industrial mass production," *IEEE J. Photovolt.*, vol. 7, no. 6, pp. 1541–1550, Nov. 2017.

[36] B. Hallam et al., "Record large-area p-type CZ production cell efficiency of 19.3% based on LDSE technology," *IEEE J. Photovolt.*, vol. 1, no. 1, pp. 43–48, Jul. 2011.

[37] S. Wang et al., "Selective emitter solar cell through simultaneous laser doping and grooving of silicon followed by self-aligned metal plating," *Sol. Energy Mater. Sol. Cells*, vol. 169, pp. 151–158, 2017, doi: 10.1016/j.solmat.2017.05.018.

[38] G. Agostinelli et al., "Very low surface recombination velocities on p-type silicon wafers passivated with a dielectric with fixed negative charge," *Sol. Energy Mater. Sol. Cells*, vol. 90, no. 18, pp. 3438–3443, 2006.

[39] B. Hoex, S. B. S. Heil, E. Langereis, M. C. M. van de Sanden, and W. M. M. Kessels, "Ultralow surface recombination of c-Si substrates passivated by plasma-assisted atomic layer deposited Al2O3," *Appl. Phys. Lett.*, vol. 89, no. 4, Jul. 2006, Art. no. 042112, doi: 10.1063/1.2240736.

[40] D. Lu et al., "Laser doping through anodic aluminium oxide layers formed on silicon solar cells," in *Proc. IEEE 21st Photovolt. Sci. Eng. Conf.*, 2011.

[41] A. Fell, E. Franklin, D. Walter, D. Suh, and K. Weber, "Laser doping from Al2O3 layers," in *Proc. 27th Eur. Photovolt. Sol. Energy Conf.*, 2012, pp. 706–708.

[42] N.-P. Harder, Y. Larionova, and R. Brendel, "Al+-doping of Si by laser ablation of Al2O3/SiN passivation," *Physica Status Solidi A*, vol. 210, no. 9, pp. 1871–1873, 2013.
[43] I. Martin et al., "Laser processing of Al2O3/a-SiCx: H stacks: A feasible solution for the rear surface of high-efficiency p-type c-Si solar cells," *Prog. Photovolt., Res. Appl.*, vol. 21, no. 5, pp. 1171–1175, 2013.
[44] B. Hallam, "High efficiency laser-doped silicon solar cells with advanced hydrogenation," Ph.D. dissertation, Univ. New South Wales, Sydney, NSW, Australia, 2014.
[45] Z. Hameiri, T. Puzzer, L. Mai, A. B. Sproul, and S. R. Wenham, "Laser induced defects in laser doped solar cells," *Prog. Photovolt., Res. Appl.*, vol. 19, no. 4, pp. 391–405, Jun. 2011, doi: 10.1002/pip.1043.
[46] M. Rauer, C. Schmiga, M. Glatthaar, and S. W. Glunz, "Alloying from screen-printed aluminum pastes containing boron additives," *IEEE J. Photovolt.*, vol. 3, no. 1, pp. 206–211, Jan. 2013.
[47] K. Tang, E. J. Øvrelid, G. Tranell, and M. Tangstad, "Thermochemical and kinetic databases for the solar cell silicon materials," in *Proc. 12th Int. Ferroalloys Congr.: Sustain. Future*, 2010, pp. 619–629, doi: 10.1007/978-3-642-02044-5_13/COVER.
[48] PV Lighthouse, "EDNA 2," 2014, [cited Aug. 12, 2022]. [Online]. Available: www.pvlighthouse.com.au
[49] P. Ortega et al., "p-type c-Si solar cells based on rear side laser processing of Al2O3/SiCx stacks," *Sol. Energy Mater. Sol. Cells*, vol. 106, pp. 80–83, Nov. 2012, doi: 10.1016/J.SOLMAT.2012.05.012.
[50] B. Steinhauser, M. B. Mansoor, U. Jäger, J. Benick, and M. Hermle, "Firing-stable PassDop passivation for screen printed n-type PERL solar cells based on a-SiNx:P," *Sol. Energy Mater. Sol. Cells*, vol. 126, pp. 96–100, Jul. 2014, doi: 10.1016/J.SOLMAT.2014.03.047.
[51] M. H. Norouzi et al., "PERC solar cells on p-type Cz-Si utilizing phosphorus-doped SiNXLayers," *IEEE J. Photovolt.*, vol. 12, no. 1, pp. 213–221, Jan. 2022.
[52] M. H. Norouzi et al., "Development and characterization of multifunctional PassDop layers for local p+-laser doping," *Energy Procedia*, vol. 124, pp. 891–900, Sep. 2017, doi: 10.1016/J.EGYPRO.2017.09.278.
[53] B. Steinhauser, U. Jäger, J. Benick, and M. Hermle, "PassDop rear side passivation based on Al2O3/a-SiCx:B stacks for p-type PERL solar cells," *Sol. Energy Mater. Sol. Cells*, vol. 131, pp. 129–133, Dec. 2014, doi: 10.1016/J.SOLMAT.2014.05.001.
[54] D. Suwito et al., "Industrially feasible rear passivation and contacting scheme for high-efficiency n-type solar cells yielding a Voc of 700 mV," *IEEE Trans. Electron Devices*, vol. 57, no. 8, pp. 2032–2036, Aug. 2010.
[55] E. Cornagliotti et al., "Large area p-type PERL cells featuring local p+ BSF formed by laser processing of ALD Al2O3 layers," *Sol. Energy Mater. Sol. Cells*, vol. 138, pp. 72–79, 2015, doi: 10.1016/j.solmat.2015.02.034.
[56] L. Mai, S. R. Wenham, B. Tjahjono, J. Ji, and Z. Shi, "New emitter design and metal contact for screen-printed solar cell front surfaces," in *Proc. IEEE 4th World Conf. Photovolt. Energy Conf.*, 2006, pp. 890–893, doi: 10.1109/WCPEC.2006.279599.
[57] K. S. Wang et al., "18.8% efficient laser-doped semiconductor fingers screen-printed silicon solar cell with light-induced plating," in *Proc. IEEE 38th Photovolt. Specialists Conf.*, 2012, pp. 1149–1153. doi: 10.1109/PVSC.2012.6317805.
[58] L. Mai, E. J. Mitchell, K. S. Wang, D. Lin, and S. Wenham, "The development of the advanced semiconductor finger solar cell," *Prog. Photovolt., Res. Appl.*, vol. 22, no. 12, pp. 1195–1203, Dec. 2014, doi: 10.1002/pip.2364.
[59] D. D. Smith, "Review of back contact silicon solar cells for low-cost application," in *Proc. 16th Eur. Photovolt. Sol. Energy Conf.*, 2000, pp. 1104–1107.
[60] R. Kopecek and J. Libal, "Towards large-scale deployment of bifacial photovoltaics," *Nature Energy*, vol. 3, no. 6, pp. 443–446, 2018, doi: 10.1038/s41560-018-0178-0.
[61] N.-P. Harder, V. Mertens, and R. Brendel, "Buried emitter solar cell structures: Decoupling of metallisation geometry and carrier collection geometry of back contacted solar cells," *Physica Status Solidi, Rapid Res. Lett.*, vol. 2, no. 4, pp. 148–150, Aug. 2008, doi: 10.1002/pssr.200802113.
[62] P. P. Altermatt et al., "Rear surface passivation of high-efficiency silicon solar cells by a floating junction," *J. Appl. Phys.*, vol. 80, no. 6, pp. 3574–3586, Sep. 1996, doi: 10.1063/1.363231.
[63] P. J. Cousins et al., "Generation 3: Improved performance at lower cost," in *Proc. IEEE 35th Photovolt. Spec. Conf.*, 2010, pp. 275–278.
[64] R. A. Sinton and R. M. Swanson, "Simplified backside-contact solar cells," *IEEE Trans. Electron Devices*, vol. 37, no. 2, pp. 348–352, Feb. 1990.
[65] M. A. Green et al., "Crystalline silicon on glass (CSG) thin-film solar cell modules," *Sol. Energy*, vol. 77, no. 6, pp. 857–863, 2004, doi: 10.1016/j.solener.2004.06.023.
[66] J.-H. Guo, "High efficiency N-type laser-grooved buried contact silicon solar cells," Ph.D. dissertation, UNSW, Sydney, NSW, Australia, 2004.
[67] R. M. Swanson, "Point-contact solar cells: Modeling and experiment," *Sol. Cells*, vol. 17, no. 1, pp. 85–118, 1986, doi: 10.1016/0379-6787(86)90061-X.
[68] W. Mulligan et al., "Manufacture of solar cells with 21% efficiency," in *Proc. 19th Eur. Photovolt. Sol. Energy Conf.*, 2004, Paper 387.
[69] P. Cousins, "Lab to GW fab for 25% back-contacted n-type cells," in *Proc. PV Cell Tech. Conf.*, 2016.
[70] "SunPower X-series solar panels," 2020. Accessed: Sep. 09, 2020. [Online]. Available: https://us.sunpower.com/solar-panels-technology/x-series-solar-panels
[71] M. Dahlinger, K. Carstens, E. Hoffmann, R. Zapf-Gottwick, and J. H. Werner, "23.2% laser processed back contact solar cell: Fabrication, characterization and modeling," *Prog. Photovolt., Res. Appl.*, vol. 25, no. 2, pp. 192–200, Feb. 2017, doi: 10.1002/pip.2854.
[72] M. Dahlinger et al., "22.0% efficient laser doped back contact solar cells," *Energy Procedia*, vol. 38, pp. 250–253, Jan. 2013, doi: 10.1016/J.EGYPRO.2013.07.274.
[73] B. Hallam, C. Chan, A. Sugianto, and S. Wenham, "Deep junction laser doping for contacting buried layers in silicon solar cells," *Sol. Energy Mater. Sol. Cells*, vol. 113, pp. 124–134, 2013, doi: 10.1016/j.solmat.2013.02.011.
[74] C. E. Chan, "Novel laser doping technology for silicon solar cells," Ph.D. dissertation, Univ. New South Wales, Sydney, NSW, Australia, 2014.
[75] C. E. Chan, B. J. Hallam, and S. R. Wenham, "Simplified interdigitated back contact solar cells," *Energy Procedia*, vol. 27, pp. 543–548, 2012, doi: 10.1016/j.egypro.2012.07.107.
[76] C.-W. Chen et al., "Modeling the potential of screen printed front junction CZ silicon solar cell with tunnel oxide passivated back contact," *Prog. Photovolt., Res. Appl.*, vol. 25, no. 1, pp. 49–57, Jan. 2017, doi: 10.1002/pip.2809.
[77] Y. Tao et al., "High-efficiency selective boron emitter formed by wet chemical etch-back for n-type screen-printed Si solar cells," *Appl. Phys. Lett.*, vol. 110, no. 2, Jan. 2017, Art. no. 21101, doi: 10.1063/1.4973626.
[78] Z. Sun and M. C. Gupta, "A study of laser-induced surface defects in silicon and impact on electrical properties," *J. Appl. Phys.*, vol. 124, no. 22, Dec. 2018, Art. no. 223103, doi: 10.1063/1.5058143.
[79] M. Abbott, P. Cousins, F. Chen, and J. Cotter, "Laser-induced defects in crystalline silicon solar cells," in *Proc. IEEE Conf. Rec. 31st Photovolt. Specialists Conf.*, 2005, pp. 1241–1244, doi: 10.1109/PVSC.2005.1488364.
[80] M. Ametowobla, G. Bilger, J. R. Köhler, and J. H. Werner, "Laser induced lifetime degradation in p-type crystalline silicon," *J. Appl. Phys.*, vol. 111, no. 11, Jun. 2012, Art. no. 114515, doi: 10.1063/1.4725191.
[81] M. Ernst, J. D. Huyeng, D. Walter, K. C. Fong, and A. Blakers, "Unravelling the origins of contact recombination for localized laser-doped contacts," in *Proc. IEEE 7th World Conf. Photovolt. Energy Convers. Joint Conf. 45th IEEE PVSC, 28th PVSEC 34th EU PVSEC*, 2018, pp. 2195–2199, doi: 10.1109/PVSC.2018.8547383.
[82] J. Müller et al., "Recombination at laser-processed local base contacts by dynamic infrared lifetime mapping," *J. Appl. Phys.*, vol. 108, no. 12, Dec. 2010, Art. no. 124513, doi: 10.1063/1.3517109.
[83] J. M. Fairfield and G. H. Schwuttke, "Silicon diodes made by laser irradiation," *Solid State Electron*, vol. 11, no. 12, Dec. 1968, Art. no. 1175-IN6, doi: 10.1016/0038-1101(68)90008-7.
[84] R. T. Young, R. F. Wood, and W. H. Christie, "Laser processing for high-efficiency Si solar cells articles you may be interested in," *J. Appl. Phys.*, vol. 53, 1982, Art. no. 1178, doi: 10.1063/1.330568.
[85] B. Hartiti, A. Slaoui, J. C. Muller, and P. Siffert, "Electrically active defects in silicon after excimer laser processing," *J. Appl. Phys.*, vol. 66, Oct. 1989, Art. no. 3934, doi: 10.1063/1.344021.
[86] A. Mesli, J. C. Muller, and P. Siffert, "Analysis and origin of point defects in silicon after liquid phase transient annealing," *Le J. de Physique Colloques*, vol. 44, no. C5, pp. C5-281–C5-295, Oct. 1983, doi: 10.1051/JPHYSCOL:1983543.
[87] A. Barhdadi, B. Hartiti, and J.-C. Muller, "Active defects generated in silicon by laser doping process," *Afr. Rev. Phys.*, vol. 6, pp. 229–238, 2011.

[88] M. Finetti, P. Negrini, S. Solmi, and D. Nobili, "Electrical properties and stability of supersaturated phosphorus-doped silicon layers," *J. Electrochem. Soc.*, vol. 128, no. 6, pp. 1313–1317, Jun. 1981, doi: 10.1149/1.2127626/XML.

[89] V. C. Lo et al., "Pulsed laser induced annealing and spin-on-doping in silicon wafers," in *Proc. IEEE Int. Conf. Semicond. Electron.*, 1997, pp. 85–88, doi: 10.1109/SMELEC.1996.616458.

[90] M. S. Skolnick, A. G. Cullis, and H. C. Webber, "Defect photoluminescence from pulsed-laser-annealed ion-implanted Si," *Appl. Phys. Lett.*, vol. 38, no. 6, Aug. 1998, Art. no. 464, doi: 10.1063/1.92405.

[91] M. S. Skolnick, A. G. Cullis, and H. C. Webber, "Defect-induced photoluminescence from pulsed laser annealed Si," *MRS Online Proc. Library*, vol. 1, no. 1, pp. 185–191, Feb. 2011, doi: 10.1557/PROC-1-185.

[92] Z. Sun and M. C. Gupta, "Laser induced defects in silicon solar cells and laser annealing," in *Proc. IEEE 43rd Photovolt. Spec. Conf.*, 2016, pp. 713–716, doi: 10.1109/PVSC.2016.7749694.

[93] Z. Sun and M. C. Gupta, "Laser annealing of silicon surface defects for photovoltaic applications," *Surf. Sci.*, vol. 652, pp. 344–349, Oct. 2016, doi: 10.1016/J.SUSC.2016.03.028.

[94] H. T. Nguyen et al., "Dislocations in laser-doped silicon detected by micro-photoluminescence spectroscopy," *Appl. Phys. Lett.*, vol. 107, no. 2, Jul. 2015, Art. no. 022101, doi: 10.1063/1.4926360.

[95] U. Besi-Vetrella et al., "Selective doping of silicon by rapid thermal and laser assisted processes," *Mater. Sci. Semicond. Process.*, vol. 1, no. 3–4, pp. 325–329, Dec. 1998, doi: 10.1016/S1369-8001(98)00026-2.

[96] A. G. Cullis, H. C. Webber, J. M. Poate, and N. G. Chew, "Tem study of silicon laser annealed after the implantation of low solubility dopants," *J. Microsc.*, vol. 118, no. 1, pp. 41–49, Jan. 1980, doi: 10.1111/J.1365-2818.1980.TB00244.X.

[97] Y. S. Liu, S. W. Chiang, and F. Bacon, "Rapid oxidation via adsorption of oxygen in laser-induced amorphous silicon," *Appl. Phys. Lett.*, vol. 38, Aug. 1981, Art. no. 1005, doi: 10.1063/1.92246.

[98] L. Liu et al., "Laser-doping technique using ultraviolet laser for shallow doping in crystalline silicon solar cell fabrication," *Jpn. J. Appl. Phys.*, vol. 48, 2009, Art. no. 71201, doi: 10.1143/JJAP.48.071201.

[99] S. Baumann, D. Kray, K. Mayer, A. Eyer, and G. P. Willeke, "Comparative study of laser induced damage in silicon wafers," in *Proc. IEEE 4th World Conf. Photovolt. Energy Convers.*, 2006, pp. 1142–1145, doi: 10.1109/WCPEC.2006.279363.

[100] Z. Sun and M. C. Gupta, "Laser processing of silicon for photovoltaics and structural phase transformation," *Appl. Surf. Sci.*, vol. 456, pp. 342–350, Oct. 2018, doi: 10.1016/J.APSUSC.2018.06.092.

[101] M. S. Amer, L. Dosser, S. LeClair, and J. F. Maguire, "Induced stresses and structural changes in silicon wafers as a result of laser micromachining," *Appl. Surf. Sci.*, vol. 187, nos. 3/4, pp. 291–296, Feb. 2002, doi: 10.1016/S0169-4332(01)01043-1.

[102] F. H. Pollak, R. Tsu, and E. Mendez, "Electrolyte electroreflectance investigation of ion-damaged laser-annealed silicon," in *Proc. Laser Electron Beam Process. Mater.*, 1979, pp. 195–200.

[103] H. S. Tan, S. C. Ng, H. S. Woon, and G. Hultquist, "Transient capacitance measurements of laser radiation-induced defects in silicon," *Semicond. Sci. Technol.*, vol. 5, no. 7, Jul. 1990, Art. no. 657, doi: 10.1088/0268-1242/5/7/004.

[104] G. A. Kachurin, E. V. Nideav, and A. I. Popov, "Laser annealing of radiation defects, studied by the capacitance spectroscopy method," *Sov. Phys. Semicond.*, vol. 16, no. 1, pp. 13–15, 1982.

[105] W. O. Adekoya, J. C. Muller, and P. Siffert, "Rapid thermal annealing of electrically-active defects in virgin and implanted silicon," *Appl. Phys. A*, vol. 42, no. 3, pp. 227–232, Mar. 1987, doi: 10.1007/BF00620605.

[106] J. L. Benton, "Post-illumination annealing of defects in laser-processed silicon," *Laser Electron Beam Process. Mater.*, pp. 430–434, 1980.

[107] J. L. Benton et al., "Hydrogen passivation of point defects in silicon," *Appl. Phys. Lett.*, vol. 36, no. 8, Jul. 2008, Art. no. 670, doi: 10.1063/1.91619.

[108] N. M. Johnson, R. B. Gold, and J. F. Gibbons, "Electronic defect levels in self-implanted cw laser-annealed silicon," *Appl. Phys. Lett.*, vol. 34, no. 10, Aug. 2008, Art. no. 704, doi: 10.1063/1.90612.

[109] K. L. Wang, Y. S. Liu, G. E. Possin, J. Karins, and J. Corbett, "Defects in Q-switched laser annealed silicon," *J. Appl. Phys.*, vol. 54, no. 7, Jun. 1983, Art. no. 3839, doi: 10.1063/1.332608.

[110] A. Mesli, J. C. Muller, D. Salles, and P. Siffert, "Origin of the defects observed after laser annealing of implanted silicon," *Appl. Phys. Lett.*, vol. 39, no. 2, Aug. 1981, Art. no. 159, doi: 10.1063/1.92646.

[111] Z. K. Fan, V. Q. Ho, and T. Sugano, "Quenched-in defects in laser annealed silicon," *Appl. Phys. Lett.*, vol. 40, no. 5, Jun. 1982, Art. no. 418, doi: 10.1063/1.93124.

[112] H. Indusekhar, V. Kumar, and D. Sengupta, "Investigation of deep defects due to α-particle irradiation in n-silicon," *Physica Status Solidi (A)*, vol. 93, no. 2, pp. 645–653, Feb. 1986, doi: 10.1002/PSSA.2210930230.

[113] L. C. Kimerling, "New developments in defect studies in semiconductors," *IEEE Trans. Nucl. Sci.*, vol. 23, no. 6, pp. 1497–1505, Dec. 1976.

[114] J. W. Chen and A. G. Milnes, "Energy levels in silicon," *Annu. Rev. Mater. Sci.*, vol. 10, no. 1, pp. 157–228, 1980.

[115] L. D. Yau and C. T. Sah, "Quenched-in centers in silicon p+n junctions," *Solid State Electron*, vol. 17, no. 2, pp. 193–201, Feb. 1974, doi: 10.1016/0038-1101(74)90067-7.

[116] Y. J. Han et al., "Low-temperature micro-photoluminescence spectroscopy on laser-doped silicon with different surface conditions," *Appl. Phys. A, Mater. Sci. Process.*, vol. 122, no. 4, pp. 1–10, Apr. 2016, doi: 10.1007/S00339-016-9926-9/FIGURES/7.

[117] J. M. Bovatsek et al., "High-speed fabrication of laser doping selective emitter solar cells using 532 nm continuous wave (cw) and modelocked quasi-cw laser sources," in *Proc. 26th Eur. Photovolt. Sol. Energy Conf. Exhib.*, 2011.

[118] A. M. Wenham et al., "Photovoltaic device structure and method," U.S. Patent 2012/0 125 424 A1, 2012.

[119] A. Sugianto, B. S. Tjahjono, J. Guo, and S. Wenham, "Impact of laser induced defects on the performance of solar cells using localised laser doped regions beneath the metal contact," in *Proc. 22nd Eur. Photovolt. Sol. Energy Conf.*, 2007, pp. 1759–1762.

[120] B. J. Hallam et al., "Overcoming the challenges of hydrogenation in silicon solar cells," *Australian J. Chem.*, vol. 71, no. 10, pp. 743–752, Sep. 2018, doi: 10.1071/CH18271.

[121] S. R. Wenham, B. Tjahjono, N. Kuepper, and A. Lennon, "Improved metallization method for silicon solar cells," World Patent 2011/050 399, 2011.

[122] A. Slaoui, A. Barhdadi, J. C. Muller, and P. Siffert, "Passivation of laser induced defects in silicon by low energy hydrogen ion implantation," *Appl. Phys. A*, vol. 39, no. 3, pp. 159–162, Mar. 1986, doi: 10.1007/BF00620729.

[123] A. M. Soufiani, A. Soeriyadi, C. Chan, and B. Hallam, "Improved laser-induced defect passivation and simultaneous elimination of light-induced degradation in p-type czochralski silicon," *IEEE J. Photovolt.*, vol. 11, no. 6, pp. 1370–1379, Nov. 2021.

[124] S. Wang et al., "Advanced passivation of laser-doped and grooved solar cells," *Sol. Energy Mater. Sol. Cells*, vol. 193, pp. 403–410, May 2019, doi: 10.1016/J.SOLMAT.2019.01.025.

[125] B. Hallam et al., "Hydrogen passivation of laser-induced defects for laser-doped silicon solar cells," *IEEE J. Photovolt.*, vol. 4, no. 6, pp. 1413–1420, Nov. 2014.

[126] L. E. Black et al., "Self-aligned local contact opening and n+ diffusion by single-step laser doping from POx/Al2O3 passivation stacks," *Sol. Energy Mater. Sol. Cells*, vol. 217, Nov. 2020, Art. no. 110717, doi: 10.1016/J.SOLMAT.2020.110717.

[127] S. Gall, B. Paviet-Salomon, J. Lerat, and T. Emeraud, "High quality passivation scheme combined with laser doping from SiN:P and SiN:B layer for silicon solar cell," *Energy Procedia*, vol. 27, pp. 467–473, Jan. 2012, doi: 10.1016/J.EGYPRO.2012.07.095.

[128] U. Jäger, D. Suwito, J. Benick, S. Janz, and R. Preu, "A laser based process for the formation of a local back surface field for n-type silicon solar cells," *Thin Solid Films*, vol. 519, no. 11, pp. 3827–3830, Mar. 2011, doi: 10.1016/J.TSF.2011.01.237.

[129] B. Paviet-Salomon et al., "Laser doping using phosphorus-doped silicon nitrides," *Energy Procedia*, vol. 8, pp. 700–705, 2011, doi: 10.1016/J.EGYPRO.2011.06.204.

[130] M. Ernst et al., "Fabrication of a 22.8% efficient back contact solar cell with localized laser-doping," *Physica Status Solidi (A)*, vol. 214, no. 11, Nov. 2017, Art. no. 1700318, doi: 10.1002/pssa.201700318.

[131] G. López et al., "Base contacts and selective emitters processed by laser doping technique for p-type IBC c-Si solar cells," *Energy Procedia*, vol. 77, pp. 752–758, 2015, doi: 10.1016/j.egypro.2015.07.106.

[132] G. Masmitja et al., "IBC c-Si(n) solar cells based on laser doping processing for selective emitter and base contact formation," *Energy Procedia*, vol. 92, pp. 956–961, 2016, doi: 10.1016/j.egypro.2016.07.107.

[133] P. Ortega et al., "Fully low temperature interdigitated back-contacted c-Si(n) solar cells based on laser-doping from dielectric stacks," *Sol. Energy Mater. Sol. Cells*, vol. 169, pp. 107–112, 2017, doi: 10.1016/j.solmat.2017.05.017.